

Study on the Durability and Mechanical Characteristic of Bumper Rail for Each of the Configurations by using Simulated Structural Analysis

¹Kye-Kwang Choi and ²Jae-Ung Cho

¹Department of Metal Mold Design Engineering,

²Division of Mechanical and Automotive Engineering, Kongju National University,
1223-24 Cheonan Daero, Seobuk-gu, Cheonan-si, 31080 Chungnam, Korea

Abstract: The bumper rail plays extremely important role in the collision of vehicles. Extent of human casualties and damages to the vehicle is determined in accordance with the extent to which the bumper rail can absorb the impact when the vehicle is involved in head-on collision. In this study, a total of five different bumper rail models are designed for each of the configurations by making reference to the commercially available bumper rails on the basis of the aforementioned function of the bumper rail. Simulated structural analysis was then executed to assess and research the durability and mechanical characteristic of each of the bumper rail models. In this study, a total of five types of bumper rail models for each of configurations were 3D modeled with CATIA design program by making reference to the commercially available bumper rails and simulated structural analysis on these models was executed. After having designed 3D bumper rail models for each of the configurations, it was possible to confirm the durability and mechanical characteristic of each of the bumper rail models by executing simulated structural analysis. As the result of this study, bumper rail model 5 is deemed to have the best durability with the higher maximum stress in comparison to other bumper rail models. Moreover, this model 5 is determined to be most appropriate for application to vehicles as it displayed the largest maximum deformation indicating the best ability to absorb the impact imparted at the time of collision of the vehicle, although, deformation and damages due to deformation under load above the prescribed level could occur. This study is on the research of the durability and mechanical characteristics of bumper rails used in automobiles. It is deemed that data obtained through the corresponding research can be utilized as the basic data for more advanced designing of and researches related to bumper rail.

Key words: Bumper rail, structural analysis, configuration, durability, mechanical characteristic, appropriate

INTRODUCTION

Nowadays, the enhanced fuel efficiency and stability are pursued for automobile with the fuel efficiency improved through the reduction in weight and cost. Bumper is a part of the automobile with the functions to protect the passengers and chassis from external impact (Park, 2011; Zeng *et al.*, 2016; Belingardi *et al.*, 2013; Chen and Liu, 2013; Wan *et al.*, 2013). The structure of the automobile bumper is generally composed of bumper cover, impact absorption material, bumper rail and chassis connector (Xu *et al.*, 2013). The materials such as steel plate, plastic and aluminum are mostly used for the manufacturing of bumper rail. Bumper rail that is connected to the bumper among the components that compose the bumper plays very important role in the collision of vehicles. Extent of human casualties and damages to the vehicle is determined by the extent of absorption of the impact by the bumper rail at the time of head-on collision of the vehicle. In this

study, a total of five different types of bumper rail models were 3D designed for each of the configurations by making reference to the commercially available bumper rails on the basis of this function of the bumper rail (Davoodi *et al.*, 2012; Magalhaes *et al.*, 2012; Tai and Zhang, 2012; Chinnadurai and Vendan, 2017; Senthilkumar and Rajasekaran, 2017). This research was conducted to assess the durability and the mechanical characteristic of each of the bumper rails by executing simulated structural analysis on the basis of the designed models. In addition, it is deemed that data obtained through the corresponding research can be utilized as the basic data for more advanced designing of and researches related to bumper rail (McCall and Balling, 2017; Le and Nakagawa, 2016).

MATERIALS AND METHODS

In this study, a total of five types of bumper rail models for each of configurations were 3D modeled with

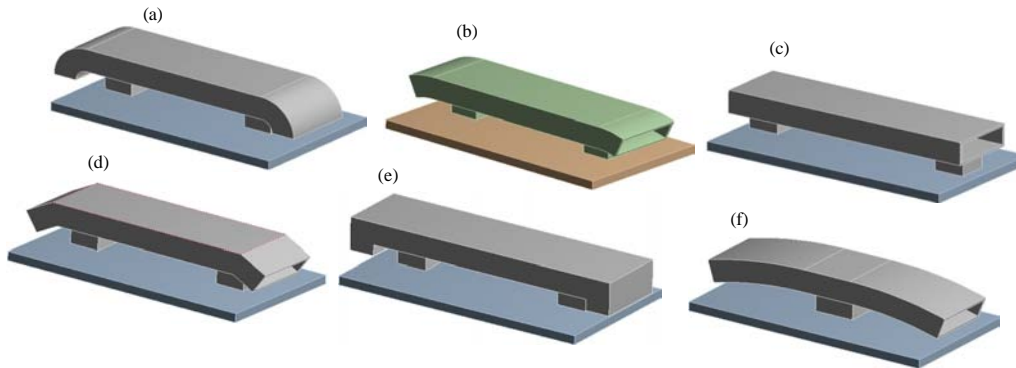


Fig. 1: Research models: a) Bumper rail model 1; b) Bumper rail model 2; c) Bumper rail model 3; d) Bumper rail model 4; e) Bumper rail model 5 and f) Bumper rail model 6

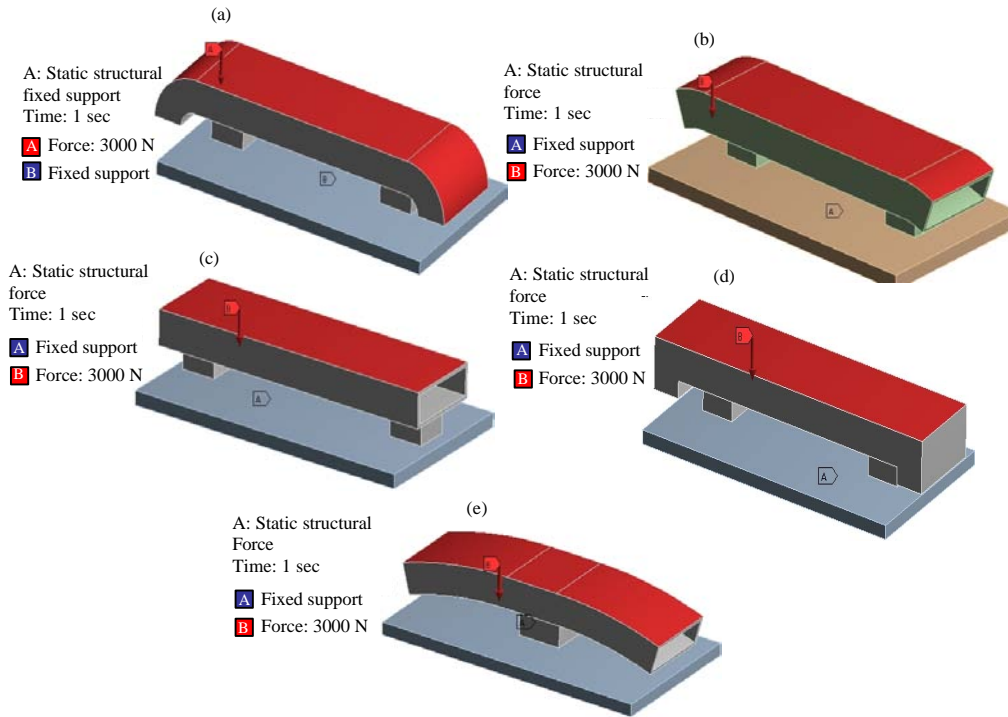


Fig. 2: Boundary conditions of bumper rail models: a) Bumper rail model 1; b) Bumper rail model 2; c) Bumper rail model 3; d) Bumper rail model 4 and e) Bumper rail model 5

CATIA design program by making reference to the commercially available bumper rails and simulated structural analysis on these models was executed. Figure 1 illustrates the appearances of the bumper rail models while Table 1 lists the material properties of the bumper rail models (Pishbin, 2016; Li *et al.*, 2016).

Table 1: Material properties

Material	Stainless steel
Density (kg/m ³)	7750
Young's modulus (GPa)	193
Poisson's ratio	0.31
Yield strength (MPa)	207
Ultimate strength (MPa)	586

Boundary conditions: Figure 2 illustrates the boundary conditions applied to each of the bumper rail models to execute simulated structural analysis. Firstly, the force condition of applying 3.000 N of load by presuming the situation in which the load is applied to the frontal portion

of the bumper rail is applied to all the bumper rail models. With the presumption that the bumper rail is fixated to the bracket that connects the bumper rail to the frame of the automobile, the fixation was made by applying fixed support conditions.

RESULTS AND DISCUSSION

Figure 3 illustrates the quantity of deformation and the resultant values of the stress that are happening in the bumper rail model 1 during the simulated structural analysis on each of the bumper rail models. As the results of the execution of structural analysis, the maximum quantity of deformation happening in the corresponding model when load of 3.000 N was applied to the frontal portion was found to be approximately 0.0382 mm while the maximum stress was found to be approximately 16.34MPa. In addition, the maximum deformation occurred in the middle of the front portion of the bumper rail model while the maximum stress occurred at the both edges of the central portion of the model. Moreover, the distribution of stress similar to the maximum stress was found in portion of the top of the bumper rail model.

Figure 4 illustrates the resultant values of the quantity of deformation and stress generated in the bumper rail model 2. As the results of the execution of analysis, it displayed the appearances that are similar to

those of the bumper rail model 1. The maximum quantity of deformation generated in the corresponding model was found to be approximately 0.0494 mm while the maximum stress was found to be approximately 18.00 MPa. In addition, similar to the bumper rail model 1, the maximum deformation occurred at the center of the front portion of the bumper rail model while the maximum stress occurred at the both edges of the central portion of the model. Furthermore, bumper rail model 2 also displayed the distribution of stress similar to the maximum stress which was found in portion of the top part, similar to those observed in the bumper rail model 1.

Figure 5 illustrates the resultant values of the quantity of deformation and stress of the bumper rail model 3. The maximum quantity of deformation happening in the corresponding model was found to be approximately 0.0604 mm while the maximum stress was approximately 21.87 MPa. In addition, the areas of the occurrence of such maximum deformation and maximum stress displayed the similarity to those of the bumper rail models explained above. As such, the maximum

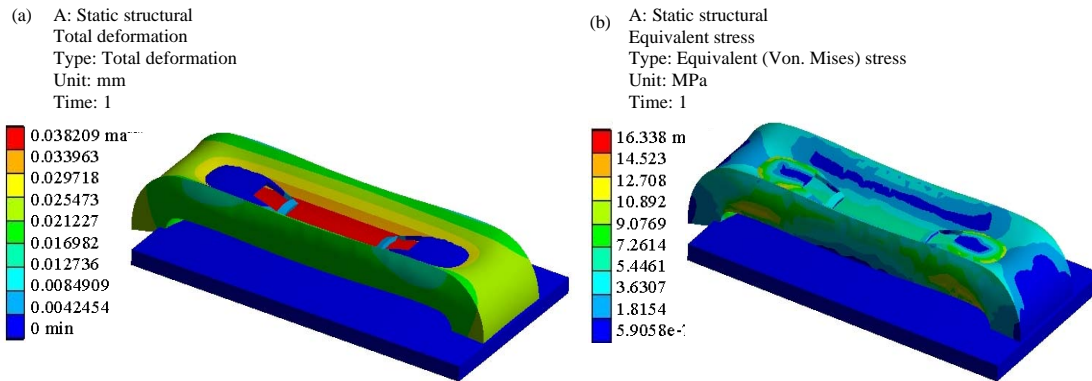


Fig. 3: a, b) Total deformation and equivalent stress of bumper rail model 1

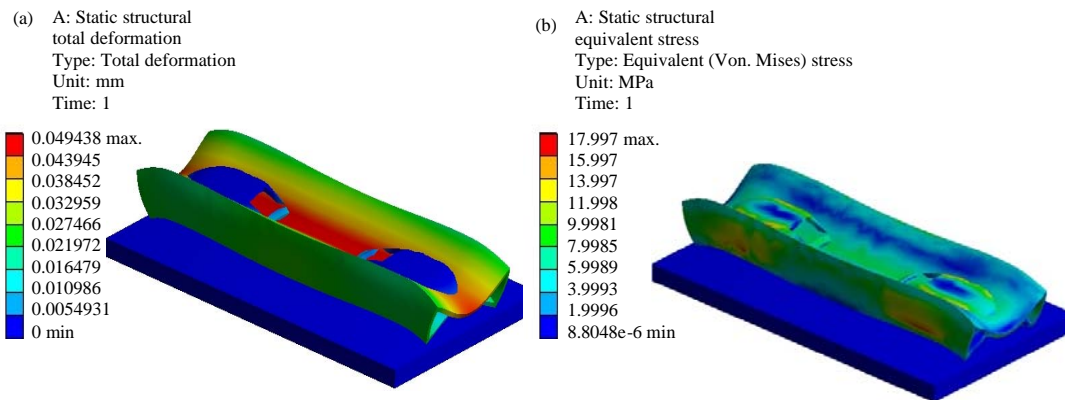


Fig. 4: a, b) Total deformation and equivalent stress of bumper rail model 2

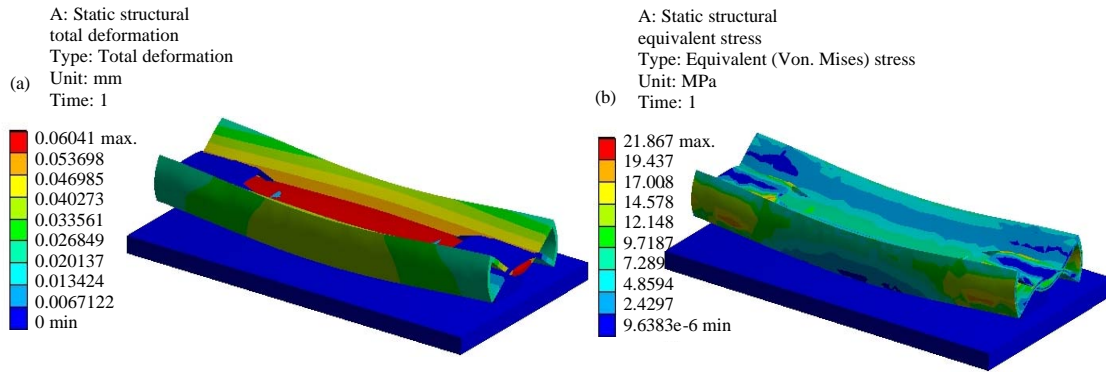


Fig. 5: a, b) Total deformation and equivalent stress of bumper rail model 3

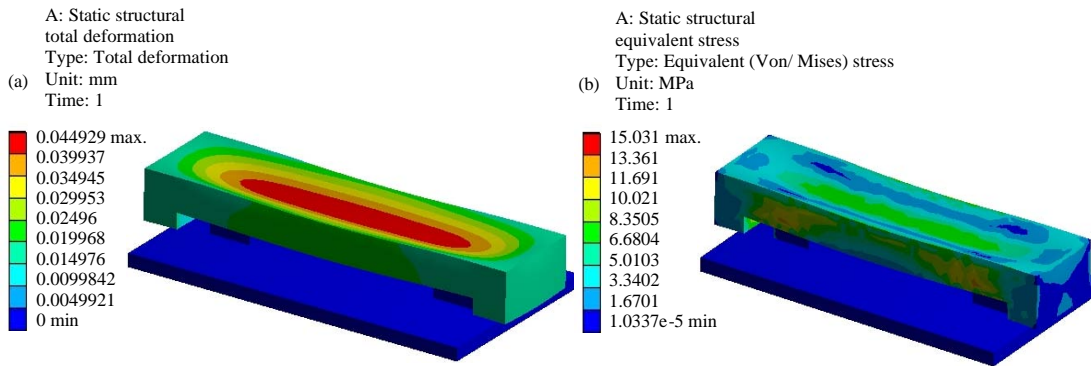


Fig. 6: a, b) Total deformation and equivalent stress of bumper rail model 4

deformation occurred at the center of the front portion of the bumper rail model while the maximum stress occurred at the both edges of the central portion of the model. Furthermore, in the case of the corresponding bumper rail model, the distribution of stress similar to the maximum stress was also found in portion of the top part.

Figure 6 illustrates the resultant values of the quantity of deformation and stress of the bumper rail model 4. The maximum quantity of deformation generated in the corresponding model was found to be approximately 0.0449 mm while the maximum stress was approximately 15.03 MPa. In addition, the maximum deformation occurred at the central portion of the frontal port of the bumper rail model with wider area in comparison to other models while the maximum stress occurred in the both edges of the central portion of the model. Moreover, it was possible to confirm the generation of stress similar to the maximum stress in portion of the top part of the corresponding model.

Figure 7 illustrates the resultant values of the quantity of deformation and stress of the bumper rail model 5. The maximum quantity of deformation generated in the corresponding model was found to be

Table 2: Comparison analysis results of bumper rail models

Models	Maximum total deformation (mm)	Maximum equivalent stress (MPa)
Bumper rail model 1	0.0382	16.34
Bumper rail model 2	0.0494	18.00
Bumper rail model 3	0.0604	21.87
Bumper rail model 4	0.0449	15.03
Bumper rail model 5	0.0856	24.34

approximately 0.0856 mm while the maximum stress was approximately 24.35 MPa. In the case of the corresponding bumper model, unlike other models in which the maximum deformation generally occur at the central portion of the frontal part of the bumper rail model, maximum deformation was generated at the both end portions. The maximum stress also occurred at the top portion, unlike other bumper rail models.

Comparison of analysis results and considerations:

Table 2 mutually compares the resultant values of the structural analysis on each of the bumper rail models. When five bumper rail models are mutually compared, the maximum quantity of deformation was approximately 0.0382 mm and maximum stress was approximately 16.34 MPa for the bumper rail model 1, maximum quantity

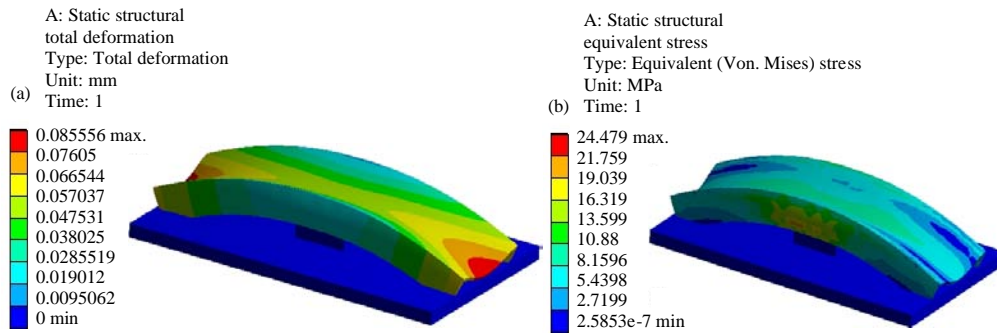


Fig. 7: a, b) Total deformation and equivalent stress of bumper rail model 5

of deformation was approximately 0.0494 mm and maximum stress was approximately 18.00 MPa for the bumper rail model 2 and maximum quantity of deformation was approximately 0.0604 mm and maximum stress was approximately 21.87 MPa for the bumper rail model 3. Moreover, it was confirmed that the maximum quantity of deformation was approximately 0.0449 mm while the maximum stress was approximately 15.03 MPa for the bumper rail model 4 and the maximum quantity of deformation was approximately 0.0856 mm and maximum stress was approximately 24.34 MPa for the bumper rail model 5. As the results of this study, bumper rail model 5 is deemed to have the best durability since it had the highest maximum stress among all the bumper rail models. Moreover, it is also determined to be most appropriate for application to vehicles, since, it can absorb the impact exerted to the vehicle at the time of collision given the highest maximum quantity of deformation among all the models, although, there could be occurrence of deformation under load in excess of prescribed level and damages due to such deformation.

CONCLUSION

In this study, the following conclusions were derived by executing simulated structural analysis for bumper rail models for each of the configurations. It was possible to confirm the durability and mechanical characteristic of each of the bumper rail models by executing simulated structural analysis after having 3D designed bumper rail models for each of the configurations.

When bumper rail models for each of five configurations were mutually compared, maximum quantity of deformation was approximately 0.0382 mm and maximum stress was approximately 16.34 MPa for the bumper rail model 1, maximum quantity of deformation was approximately 0.0494 mm and maximum stress was approximately 18.00 MPa for the bumper rail model 2 and

maximum quantity of deformation was approximately 0.0604 mm and maximum stress was approximately 21.87 MPa for the bumper rail model 3. Moreover, it was confirmed that the maximum quantity of deformation was approximately 0.0449 mm while the maximum stress was approximately 15.03 MPa for the bumper rail model 4 and the maximum quantity of deformation was approximately 0.0856 mm and maximum stress was approximately 24.34 MPa for the bumper rail model 5.

As the results of this study, bumper rail model 5 is deemed to have the best durability since it had the highest maximum stress among all the bumper rail models. Moreover, it is also determined to be most appropriate for application to vehicles since it can absorb the impact exerted to the vehicle at the time of collision given the highest maximum quantity of deformation among all the models, although there could be occurrence of deformation under load in excess of prescribed level and damages due to such deformation.

This study was on the research of the durability and mechanical characteristics of bumper rails applied to automobile. It is deemed that data obtained through the corresponding research can be utilized as the basic data for more advanced designing of and researches related to bumper rails.

REFERENCES

- Belingardi, G., A.T. Beyene and E.G. Koricho, 2013. Geometrical optimization of bumper beam profile made of pultruded composite by numerical simulation. *Compos. Struct.*, 102: 217-225.
- Chen, F.K. and S.W. Liu, 2013. Die Compensation Design for Stamping a High Strength Automotive Bumper Inner. In: *Advanced Materials Research*, Xianghua, L., Z. Kaifeng and L. Mingzhe (Eds.). Trans Tech Publications, Switzerland, pp: 796-799.

- Chinnadurai, T. and S.A. Vendan, 2017. Thermal and structural analysis of ultrasonic-welded PC-ABS blend for automobile applications. *J. Therm. Anal. Calorim.*, 127: 1995-2003.
- Davoodi, M.M., S.M. Sapuan, A. Ali and D. Ahmad, 2012. Effect of the strengthened ribs in hybrid toughened kenaf-glass epoxy composite bumper beam. *Life Sci. J.*, 9: 285-289.
- Le, A.D. and M. Nakagawa, 2016. A system for recognizing online handwritten mathematical expressions by using improved structural analysis. *Intl. J. Doc. Anal. Recognit.*, 19: 305-319.
- Li, J.C., X.W. Chen and F.L. Huang, 2016. FEM analysis on the deformation and failure of fiber reinforced metallic glass matrix composite. *Mater. Sci. Eng. A.*, 652: 145-166.
- Magalhaes, R.R., C.H. Fontes and D.M.S.A. Vieira, 2012. Failure analysis and design of a front bumper using finite element method along with durability and rig tests. *Intl. J. Veh. Des.*, 60: 71-83.
- McCall, A.J. and R.J. Balling, 2017. Structural analysis and optimization of tall buildings connected with skybridges and atria. *Struct. Multidiscip. Optim.*, 55: 583-600.
- Park, D.K., 2011. A development of simple analysis model on bumper barrier impact and new IIHS bumper impact using the dynamically equivalent beam approach. *J. Mech. Sci. Technol.*, 25: 3107-3114.
- Pishbin, S., 2016. Numerical solution and structural analysis of two-dimensional integral-algebraic equations. *Numer. Algorithms*, 73: 305-322.
- Senthilkumar, B. and R. Rajasekaran, 2017. Analysis of the structural stability among cyclotide members through cystine knot fold that underpins its potential use as a drug scaffold. *Intl. J. Pept. Res. Ther.*, 23: 1-11.
- Tai, Q. and X.Y. Zhang, 2012. Research and Application on Automotive Aluminum Bumper Based on Topology Optimization. In: *Applied Mechanics and Materials*, Xiancan D. and H. Yoshinori (Eds.). Trans Tech Publications, Switzerland, pp: 495-499.
- Wan, X., X. Zhi, Q. Zhao, G. Wang and X. Xu, 2013. Concept Analysis of Automotive Aluminium Alloy Bumper. In: *Lecture Notes in Electrical Engineering*, Sae-China, F. (Ed.). Springer, Berlin, Germany, ISBN:978-3-642-33737-6, pp: 1089-1199.
- Xu, Z., X. Xu, X. Wan, Z. Zhang and Y. Li, 2013. Structure optimal design of aluminum alloy bumper anticollision beam. *Chin. J. Mech. Eng.*, 49: 136-142.
- Zeng, F., H. Xie, Q. Liu, F. Li and W. Tan, 2016. Design and optimization of a new composite bumper beam in high-speed frontal crashes. *Struct. Multidiscip. Optim.*, 53: 115-122.